Ka-Veng Yuen
Division of Engineering
and Applied Science,
California Institute of Technology,
Pasadena, CA 91125

Lambros S. Katafygiotis
Department of Civil Engineering,
Hong Kong University of Science
and Technology,
Clear Water Bay,
Kowloon, Hong Kong

Costas Papadimitriou
Department of Mechanical
and Industrial Engineering,
University of Thessaly,
Pedion Areos,
GR-38334, Volos, Greece

Neil C. Mickleborough
Department of Civil Engineering,
Hong Kong University of Science
and Technology,
Clear Water Bay,
Kowloon, Hong Kong

Optimal Sensor Placement Methodology for Identification with Unmeasured Excitation

A methodology is presented for designing cost-effective optimal sensor configurations for structural model updating and health monitoring purposes. The optimal sensor configuration is selected such that the resulting measured data are most informative about the condition of the structure. This selection is based on an information entropy measure of the uncertainty in the model parameter estimates obtained using a statistical system identification method. The methodology is developed for the uncertain excitation case encountered in practical applications for which data are to be taken either from ambient vibration tests or from other uncertain excitations such as earthquake and wind. Important issues related to robustness of the optimal sensor configuration to uncertainties in the structural model are addressed. The theoretical developments are illustrated by designing the optimal configuration for a simple 8-DOF chain-like model of a structure subjected to an unmeasured base excitation and a 40-DOF truss model subjected to wind/earthquake excitation. [DOI: 10.1115/1.1410929]

Keywords: System Identification, Health Monitoring, Sensor Placement, Information Entropy, Ambient Vibration

1 Introduction

The problem of identification of the model parameters for a structural model using dynamic data has received much attention over the years because of its importance in structural model updating, structural health monitoring and structural control. The estimate of the parameter values involves uncertainties which are due to limitations of the mathematical models used to represent the behavior of the real structure, the presence of measurement error in the data, and insufficient excitation and response bandwidth. In particular, the quality of information that the data give on the model parameters depends on the number and location of sensors in the structure. The objective of this study is to develop optimal instrumentation strategies for selecting the optimal number and location of sensors such that the resulting measured data are most informative about the condition of the structure as specified by the values of the model parameters.

An experienced engineer can make use of an optimal instrumentation strategy in order to select the number and location of sensors for the experimental design of new and complex structures where little or no experience is available such as, for example, the international space station or other space structures that may have very large size and flexibility and/or operate in microgravity environments. For conventional structures usually encountered in structural dynamic applications, an optimal instrumentation strategy provides valuable information and guidance to the less experienced engineers for the selection of appropriate sensor locations, evaluation of the capabilities and, if necessary, upgrading of an existing instrumentation.

Previous work addressing the issue of optimally locating a given number of sensors in a structure has been carried out by several investigators (e.g. [1–4]). In particular, statistical-based approaches have been developed to provide rational solutions to several issues encountered in the problem of selecting the optimal sensor and actuator configuration. Udwadia [5] proposed that the sensor configuration which maximizes some norm of the Fisher information matrix be taken as the optimal configuration. Heredia-Zanoni and Esteva [6] have extended this work to treat the case of large model uncertainties expected in model updating. They proposed that the optimal sensor configuration should be chosen as the one which minimizes the expected Bayesian loss function involving the trace of the inverse of the Fisher information matrix for each model. Both approaches deal with the issue of optimally locating a given number of sensors in a structure.

Papadimitriou et al. [7] introduced the information entropy [8] as the measure of uncertainties that best corresponds to the objective of structural testing, which is to minimize the uncertainty in the model parameters. Specifically, the optimal sensor configuration is selected as the one which minimizes the information entropy measure which is a direct measure of this uncertainty. In particular, this entropy-based measure resolved the issue related to the arbitrariness in selecting an appropriate measure for the Fisher information matrix in previous approaches based on the Fisher information matrix. However, the important advantage of the information entropy measure is that it allows us to make comparisons between sensor and actuator configurations involving a different number of sensors in each configuration. This is particularly useful for trading-off cost of instrumentation with information gained from additional sensors about the state of a structure, thus making cost-effective decisions regarding optimal instrumentation.

The present study develops optimal instrumentation strategies for the case of uncertain excitation often encountered in practical applications for which data are to be taken either from ambient vibration tests or from other uncertain excitations such as an earthquake or wind (e.g. [9–11]). The uncertainties in the model parameters is computed by extending a Bayesian statistical methodology recently proposed by Katafygiotis and Yuen [11] to handle the case of ambient data. A general information entropy-based framework is presented and several important issues encountered in the selection of the optimal sensor configuration are addressed, including issues related to the sensitivity of the optimal configuration to the number of observable modes, number of available sensors, type of structural model parametrization, and

Contributed by the Dynamic Systems and Control Division for publication in the JOURNAL OF DYNAMIC SYSTEMS, MEASUREMENT, AND CONTROL. Manuscript received by the Dynamic Systems and Control Division February 7, 2001. Associate Editor: S. Fassois.

robustness to large model uncertainties due to future damage expected in health monitoring applications. The theoretical developments are illustrated by designing the optimal configuration for a simple 8-DOF chain-like model of a structure subjected to an unmeasured base excitation and a 40-DOF truss model subjected to wind/earthquake excitation.

2 System Identification for Uncertain Excitation

2.1 Bayesian Formulation. Consider a parameterized class of structural models (e.g., a class of finite-element models) chosen to describe the input-output behavior of a structure and a parameterized class of stochastic excitation models (e.g., a class of stochastic processes) chosen to describe the spectral structure of the unmeasured excitations, respectively. Let $\boldsymbol{\theta}$ and ϕ be, respectively, the structural model and excitation model parameters that need to be assigned values in order to choose a particular model from the set of all possible models within the two model classes. Let the sampled time history $\mathbf{z}(m;\boldsymbol{\phi})$, $m=1,\cdots,N$, be a specific realization of stochastic excitation model corresponding to a specific value ϕ of the excitation model parameters, and let $\mathbf{x}(m;\boldsymbol{\theta},\phi)$, $m=1,\cdots,N$ be the corresponding sampled response time history obtained from a specific structural model specified by the value $\boldsymbol{\theta}$ of the structural model parameters. Herein, m denotes the time index at time $t_m=m\Delta t$, Δt is a prescribed sampling interval, and N is the number of sampled data.

Dynamic test data $\mathcal{D}$ obtained from the structure are used to give information for the structural and excitation model parameters $\boldsymbol{\theta}$ and ϕ, respectively. These data consist of sampled output time histories $\mathbf{y}(m)\in\mathbb{R}^{N_0}$, $m=1,\ldots,N$, at N_0 observed degrees of freedom (DOF) of the structural model. The departure between the measured response data and the response from a particular model measures the prediction error from this model and it is due to measurement noise and modeling error. A stochastic embedding approach [12] is employed according to which this difference between the measured and the model response time histories is considered to be a specific realization of a stochastic process taken from a class of probabilistic models, parameterized by the parameter set ψ. Letting $\mathbf{n}(m;\boldsymbol{\psi})$ be the prediction error at time $m\Delta t$, the observed data $\mathbf{y}(m)=[y^{(1)}(m),\ldots,y^{(N_0)}(m)]^T$ satisfies:

$$\mathbf{y}(m)=\mathbf{L}_0(\boldsymbol{\delta})\mathbf{x}(m;\boldsymbol{\theta},\boldsymbol{\phi})+\mathbf{n}(m;\boldsymbol{\psi}),\quad m=1,\cdots,N \tag{1}$$

where $\mathbf{L}_0(\boldsymbol{\delta})\in\mathbb{R}^{N_0\times N_d}$ is the observation matrix comprised of zeros and ones that selects the N_0 DOFs where measurements are made; $\boldsymbol{\delta}$ is the sensor configuration vector of dimension N_d comprised of zeros and ones with the position of the nonzero elements in $\boldsymbol{\delta}$ specifying the corresponding N_0 DOFs that are measured.

The class $\mathcal{M}$ of structural, excitation, and prediction error models, specifying the modeling assumption used in the description of the system, is thus parameterized by the set $\mathbf{a}=(\boldsymbol{\theta},\boldsymbol{\phi},\boldsymbol{\psi})$. The objective of the statistical system identification methodology is to update the values of the parameter set and their associated uncertainty using the measured test data. Herein, uncertainty in the values of the parameter set is quantified using probability density functions (PDF) which measure the relative plausibilities of each of the models in $\mathcal{M}$ specified by the parameter set $\mathbf{a}$. The selection of parameter uncertainty prior to the collection of data is based on engineering experience and is quantified by the initial PDF $p(\mathbf{a}|\mathcal{M})=\pi(\mathbf{a})$. Using Bayes' theorem, this PDF is converted to an updated PDF, $p(\mathbf{a}|\mathcal{D},\boldsymbol{\delta},\mathcal{M})$, which gives the relative plausibilities of the models based on the inclusion of the measured data, $\mathcal{D}$, as

$$p(\mathbf{a}|\mathcal{D},\boldsymbol{\delta},\mathcal{M})=kp(\mathcal{D}|\mathbf{a},\boldsymbol{\delta},\mathcal{M})\pi(\mathbf{a}) \tag{2}$$

where k is a normalizing constant, and $p(\mathcal{D}|\mathbf{a},\boldsymbol{\delta},\mathcal{M})$ accounts for the measured data and depends on the chosen class of models $\mathcal{M}$.

The optimal model $\hat{\mathbf{a}}$ within the set of all possible models $\mathbf{a}$ in the class $\mathcal{M}$ is simply the most probable model obtained by maximizing (2) or, equivalently, minimizing

$$g(\mathbf{a})=-\ln[p(\mathbf{a}|\mathcal{D},\boldsymbol{\delta},\mathcal{M})] \tag{3}$$

The most probable $\hat{\mathbf{a}}\equiv\hat{\mathbf{a}}(\boldsymbol{\delta},\mathcal{D},\mathcal{M})$ depends on the class $\mathcal{M}$ of models, the available data $\mathcal{D}$ and the sensor configuration $\boldsymbol{\delta}$. Finally, a single measure of the uncertainty in the estimate of $\mathbf{a}$ is provided by the information entropy given by [7]:

$$H_{\mathbf{a}}(\mathcal{D},\boldsymbol{\delta},\mathcal{M})=E_{\mathbf{a}}[-\ln p(\mathbf{a}|\mathcal{D},\boldsymbol{\delta},\mathcal{M})] \tag{4}$$

where $E_{\mathbf{a}}$ denotes mathematical expectation with respect to $\mathbf{a}$. This information entropy will be used later for the design of an effective sensor configuration. Herein, we adopt the formulation developed by Katafygiotis and Yuen [11] and derive the updated PDF $p(\mathbf{a}|\mathcal{D},\boldsymbol{\delta},\mathcal{M})$, needed in (4), for the general case of uncertain excitation. This formulation is based on the cross-spectral density estimates obtained from the measured data $\mathcal{D}$ and depends on the class of structural, excitation and prediction error models chosen to describe the system. Next, the selection of these classes is first presented followed by the formulation for the updated PDF $p(\mathbf{a}|\mathcal{D},\boldsymbol{\delta},\mathcal{M})$.

2.2 Class of Structural, Excitation and Prediction-Error Models. In this study, we consider the class of linear structural models with equation of motion given by

$$\mathbf{M}(\boldsymbol{\theta})\ddot{\mathbf{x}}+\mathbf{C}(\boldsymbol{\theta})\dot{\mathbf{x}}+\mathbf{K}(\boldsymbol{\theta})\mathbf{x}=\mathbf{V}^T\mathbf{g}(t) \tag{5}$$

where $\mathbf{M}(\boldsymbol{\theta})\in\mathbb{R}^{N_d\times N_d}$, $\mathbf{C}(\boldsymbol{\theta})\in\mathbb{R}^{N_d\times N_d}$ and $\mathbf{K}(\boldsymbol{\theta})\in\mathbb{R}^{N_d\times N_d}$ are, respectively, the mass, damping, and stiffness matrices of the structure which depend on the structural model parameter set $\boldsymbol{\theta}$,$\mathbf{g}(t)\in\mathbb{R}^{N_e}$ is the excitation, and $\mathbf{V}\in\mathbb{R}^{N_e\times N_d}$ is a matrix that associates the elements of the forcing vector $\mathbf{g}(t)$ to the DOFs that are excited externally. Assuming classically damped modes, the response can also be expressed in the modal space in terms of a set of modal coordinates $\mathbf{q}=[q_1,\cdots,q_{N_m}]^T$ as

$$\mathbf{x}(t)=\boldsymbol{\Phi}\mathbf{q}(t) \tag{6}$$

where $\boldsymbol{\Phi}\in\mathbb{R}^{N_d\times N_m}$ is the modeshape matrix, and $N_m(N_m\leqslant N_d)$ is the number of contributing modes. The rth modal coordinate $q_r(t)$ satisfies the modal equation

$$\ddot{q}_r(t)+2\zeta_r\omega_r\dot{q}_r(t)+\omega_r^2q_r(t)=f_r(t),\quad r=1,\ldots,N_m \tag{7}$$

where ω_r and ζ_r are the modal frequency and damping ratio, respectively, and $\mathbf{f}=[f_1,\cdots,f_{N_m}]^T$ is the modal forcing vector given by $\mathbf{f}(t)=(\mathbf{V}\boldsymbol{\Phi})^T\mathbf{g}(t)$. The modeshape matrix $\boldsymbol{\Phi}$ is taken to be mass normalized, i.e., $\boldsymbol{\Phi}^T\mathbf{M}\boldsymbol{\Phi}=\mathbf{I}$, where $\mathbf{I}$ is the identity matrix. Note that the modal frequencies, modal damping ratios and modeshapes will also depend on the structural parameters $\boldsymbol{\theta}$. For notational simplicity, this dependence will not be shown explicitly in the analysis that follows.

The probability model for the unknown excitation $\mathbf{g}(t)$ is chosen to be a stationary zero-mean Gaussian stochastic process with spectral density matrix $\mathbf{S}_{\mathbf{g}}(\omega;\boldsymbol{\phi})$, where $\boldsymbol{\phi}$ are the excitation parameters specifying the intensity and the frequency content characteristics of the stochastic excitation process. The spectral density matrices of the modal forces $\mathbf{f}(t)$ and the excitation $\mathbf{g}(t)$ are related as follows:

$$\mathbf{S}_f(\omega;\boldsymbol{\theta},\phi)=(\mathbf{V}\boldsymbol{\Phi})^T\mathbf{S}_{\mathbf{g}}(\omega;\boldsymbol{\phi})(\mathbf{V}\boldsymbol{\Phi}) \tag{8}$$

In particular, for the case of a zero-mean white noise process the excitation spectral density matrix is constant given by $\mathbf{S}_{\mathbf{g}}(\omega;\boldsymbol{\phi})=\mathbf{S}_{\mathbf{g}0}(\boldsymbol{\phi})$. In this case, the parameter vector $\boldsymbol{\phi}$ is comprised of the elements of the upper right triangle of the matrix $\mathbf{S}_{\mathbf{g}0}$. This model is an adequate approximation if the unmeasured input time excitations are sufficiently broadband over the frequency range of interest. This is the case usually encountered in ambient vibration tests.

The probabilistic model for the prediction error $\mathbf{n}(m;\boldsymbol{\phi})$, $m=1,\ldots,N$ is chosen to be a zero-mean Gaussian white noise

vector process with constant covariance matrix $\mathbf{\Sigma}_n$. The parameter vector ψ is comprised of the elements of the upper right triangle of $\mathbf{\Sigma}_n$.

2.3 Identification Based on Cross-Spectral Estimates of the Data. Consider the discrete vector process $\mathbf{y}(m) = [y^{(1)}(m), \ldots, y^{(N_0)}(m)]^T$, $m = 1, \ldots, N$, and the discrete estimator $\mathbf{S}_{y,N}(\omega_k) = [S_{y,N}^{(j,l)}(\omega_k)]$ of its cross-spectral density matrix with its (j,l) element given by:

$$S_{y,N}^{(j,l)}(\omega_k) = \frac{\Delta t}{2\pi N} \sum_{m,p=0}^{N-1} y^{(j)}(m) y^{(l)}(p) e^{-i\omega_k(p-m)\Delta t} \tag{9}$$

where $\omega_k = k\Delta\omega$, $k = 0, \ldots, N_1 - 1$ with $N_1 = \mathrm{INT}[(N+1)/2]$, $\Delta\omega = 2\pi/T$, and $T = N\Delta t$. Given M sets of observed discrete data, one may calculate for each set using (9) the corresponding estimates of the cross-spectral density matrices $\mathbf{S}_{y,N}^{(\rho)}$, $\rho = 1, \ldots, M$. The data set $\mathcal{D}$ used in the identification of the system consist of the average estimates of the spectral density obtained from the M sets of data, i.e., $\mathcal{D} = \{\mathbf{S}_{y,N}^{M}(k_1\Delta\omega), \ldots, \mathbf{S}_{y,N}^{M}(k_2\Delta\omega)\}$, where $\mathbf{S}_{y,N}^{M}(\omega_k) = 1/M \Sigma_{\rho=1}^{M} \mathbf{S}_{y,N}^{(\rho)}(\omega_k)$ is the average spectral density estimate at frequency ω_k. The expression for $p(\mathcal{D}|\mathbf{a},\boldsymbol{\delta},\mathcal{M})$ in (2) based on the cross-spectral density estimates of the data has been obtained by Yuen [13] and Katafygiotis and Yuen [11]. For completeness, the main steps of the analysis are outlined next.

Using the fact that the response of a linear system to Gaussian excitation is also Gaussian, it can be shown by Krishnaiah [14] that as $N \to \infty$, the PDF $p(\mathbf{S}_{y,N}^{M}(\omega_k)|\mathbf{a})$ asymptotically tends to a complex central Wishart distribution of dimension N_0 with M degrees of freedom and mean $E[\mathbf{S}_{y,N}(\omega_k)|\mathbf{a}]$, i.e.,

$$p(\mathbf{S}_{y,N}^{M}(\omega_k)|\mathbf{a},\boldsymbol{\delta},\mathcal{M}) \simeq \frac{\nu |\mathbf{S}_{y,N}^{M}(\omega_k)|^{M-N_0}}{[\mu_k(\mathbf{a})]^M} \times \exp\{-M \mathrm{tr}[\boldsymbol{\lambda}_k(\mathbf{a}) \mathbf{S}_{y,N}^{M}(\omega_k)]\} \tag{10}$$

where

$$\mu_k(\mathbf{a}) = |E[\mathbf{S}_{y,N}(\omega_k)|\mathbf{a}]| \tag{11}$$

$$\lambda_k(\mathbf{a}) = (E[\mathbf{S}_{y,N}(\omega_k)|\mathbf{a}])^{-1} \tag{12}$$

and $\nu = M^{M-N_0}N_0^2/[\pi^{N_0(N_0-1)/2} \Pi_{p=1}^{N_0}(M-p)!]$. The elements of $E[\mathbf{S}_{y,N}(\omega_k)|\mathbf{a}]$, denoting the expectation of the spectral density estimator, are calculated using the class $\mathcal{M}$ of models. Specifically, substituting (1) into (9) and using (6) for a given model $\mathbf{a}$, the expectation of the estimator $\mathbf{S}_{y,N}(\omega_k)$ for finite N has the form:

$$E[\mathbf{S}_{y,N}(\omega_k)|\mathbf{a}] = (\mathbf{L}_0\mathbf{\Phi}) E[\mathbf{S}_{q,N}(\omega_k)|\mathbf{a}] (\mathbf{L}_0\mathbf{\Phi})^T + E[\mathbf{S}_{n,N}(\omega_k)] \tag{13}$$

where $\mathbf{S}_{q,N}(\omega_k)$ and $\mathbf{S}_{n,N}(\omega_k)$ are the estimators of the spectral density matrices of the discrete vector processes $\mathbf{q}$ and $\mathbf{n}$, respectively, defined in analogy to (9). It can be readily shown that $E[\mathbf{S}_{n,N}(\omega_k)] \equiv \mathbf{S}_{n0} = \Delta t/(2\pi)\Sigma_n$. Also, $E[\mathbf{S}_{q,N}(\omega_k)|\mathbf{a}]$ can be calculated from the following expression [11]:

$$E[S_{q,N}^{(r,s)}(\omega_k)|\mathbf{a}] = \frac{\Delta t}{4\pi N} \sum_{m=0}^{N-1} \gamma_m [R_q^{(r,s)}(m\Delta t|\mathbf{a}) e^{-i\omega_k m\Delta t} + R_q^{(s,r)}(m\Delta t|\mathbf{a}) e^{i\omega_k m\Delta t}] \tag{14}$$

where $\gamma_0 = N$ and $\gamma_m = 2(N-m)$ for $m \geqslant 1$, and the correlation function $R_q^{(r,s)}(t|\mathbf{a})$ between the responses of modes r and s is given by:

$$R_q^{(r,s)}(t) = \int_{-\infty}^{\infty} \frac{S_f^{(r,s)}(\omega;\boldsymbol{\theta},\phi)\omega^\alpha e^{i\omega t} d\omega}{[(\omega_r^2 - \omega^2) + 2i\omega\omega_r\zeta_r][(\omega_s^2 - \omega^2) - 2i\omega\omega_s\zeta_s]} \tag{15}$$

The variable α takes the values 0, 2, or 4 depending on whether the response corresponds to displacements, velocities or accelerations, respectively. Note that the sum in the right-hand side of (14) can be calculated very efficiently using FFT.

Furthermore, it can be shown that asymptotically, as $N \to \infty$, the random matrices $\mathbf{S}_{y,N}^{M}(\omega_k)$ and $\mathbf{S}_{y,N}^{M}(\omega_l)$, evaluated, respectively, at frequencies ω_k and ω_l with $k \neq l$, are uncorrelated [13]. Wishart distributions posses the same property as normal distributions, namely, uncorrelated Wishart random matrices are independent. For finite N, it has been verified using simulations that the Wishart distribution of $\mathbf{S}_{y,N}^{M}(\omega_k)$ and the independence of the random matrices $\mathbf{S}_{y,N}^{M}(\omega_k)$ and $\mathbf{S}_{y,N}^{M}(\omega_l)$ with $k \neq l$ are good approximation as long as ω_k and ω_l belong to a certain frequency range, i.e. as long as $k,l \in [k_1, \ldots, k_2]$. For displacement measurements $k_1 = 1$ and $k_2 \ll N_1$, while for acceleration measurements $k_1 \gg 1$ and $k_2 = N_1 - 1$ [11,13]. Thus, one can assume that the random set $\mathcal{D} = \{\mathbf{S}_{y,N}^{M}(k_1\Delta\omega), \ldots, \mathbf{S}_{y,N}^{M}(k_2\Delta\omega)\}$ has all its elements approximately independently Wishart distributed. Therefore, the joint PDF $p(\mathcal{D}|\mathbf{a},\boldsymbol{\delta},\mathcal{M})$ of the data $\mathcal{D}$ can be approximated as follows:

$$p(\mathcal{D}|\mathbf{a},\boldsymbol{\delta},\mathcal{M}) \simeq \prod_{k=k_1}^{k_2} p(\mathbf{S}_{y,n}^{M}(\omega_k)|\mathbf{a}) \tag{16}$$

where each factor in the above product is given by (10).

The methodology requires only calculation of the inverse of $E[\mathbf{S}_{y,N}(\omega_k)|\mathbf{a}]$ with dimension $N_0 \times N_0$. In practice, the number of sensors N_0 is relatively small (usually less than 100) and, therefore, this inverse does not cause significant computational difficulties. The computational effort grows only linearly with the number of data points N. This is because the range of frequencies included in the analysis is fixed. However, $\Delta\omega$ is inversely proportional to N. Therefore, the number of frequency points considered, and thus the computational effort, increases linearly with N.

2.4 Approximation for Large Number of Data. The most probable parameters $\hat{\mathbf{a}}$ are obtained by minimizing (3) with $p(\mathcal{D}|\mathbf{a},\boldsymbol{\delta},\mathcal{M})$ given by (16). Furthermore, the updated PDF of the parameters $\mathbf{a}$ can be approximated [11] by a Gaussian distribution $N(\hat{\mathbf{a}},\hat{\mathbf{Q}}^{-1})$ with mean $\hat{\mathbf{a}} \equiv \hat{\mathbf{a}}(\boldsymbol{\delta},\mathcal{D})$ and covariance matrix $\hat{\mathbf{Q}}^{-1} \equiv \hat{\mathbf{Q}}^{-1}(\boldsymbol{\delta},\hat{\mathbf{a}},\mathcal{D})$, where $\hat{\mathbf{Q}}(\boldsymbol{\delta},\hat{\mathbf{a}},\mathcal{D})$ denotes the Hessian of $g(\mathbf{a})$ calculated at $\hat{\mathbf{a}}$. The (j,l) element of the Hessian matrix $\hat{\mathbf{Q}}(\boldsymbol{\delta},\hat{\mathbf{a}},\mathcal{D})$ is given by:

$$\begin{aligned} \hat{Q}^{(j,l)}(\boldsymbol{\delta},\hat{\mathbf{a}},\mathcal{D}) &= -\left[\frac{\partial^2}{\partial a_j \partial a_l} \ln[p(\mathbf{a}|\mathcal{D},\boldsymbol{\delta},\mathcal{M})]\right]_{\mathbf{a}=\hat{\mathbf{a}}} \\ &= M \sum_{k=k_1}^{k_2} \left[\frac{\partial^2}{\partial a_j \partial a_l} \left\{\mathrm{tr}[\boldsymbol{\lambda}_k(\mathbf{a}) \mathbf{S}_{y,N}^{M}(\omega_k)] + \ln \mu_k(\mathbf{a})\right\}\right]_{\mathbf{a}=\hat{\mathbf{a}}} \end{aligned} \tag{17}$$

where the last equality is valid only for a noninformative prior distribution $\pi(\mathbf{a}) = const$ over the range of parameter values of interest. Consequently, the information entropy defined in (4) takes the simplified form

$$H_{\mathbf{a}}(\boldsymbol{\delta},\mathcal{D},\mathcal{M}) = \frac{1}{2} N_a [\ln(2\pi) + 1] - \frac{1}{2} \ln\det \hat{\mathbf{Q}}(\boldsymbol{\delta},\hat{\mathbf{a}},\mathcal{D}) \tag{18}$$

3 Optimal Sensor Configuration Methodology

In a system identification methodology, the information about the condition of the system is provided by the measured data. The quality of the information depends on the sensor configuration which clearly affects the updated PDF $p(\mathbf{a}|\mathcal{D},\boldsymbol{\delta},\mathcal{M})$ of the model parameters and, consequently, the uncertainty in the parameter estimates. The sensor configuration should be selected such that the resulting measured data are most informative about the condition of the structure or, equivalently, the uncertainty in the param-

eter estimates is the least possible. Using the information entropy, defined in (4) as a single measure of the uncertainty in the model parameters, the optimal sensor configuration should be selected as the one which minimizes the information entropy measure. Although this is a well-posed optimization problem, there is a major complication arising from the explicit dependence of the information entropy on the data which are not available in the initial stage of designing the experiment. This complication can be overcome by considering the limiting case of large data ($M,N\to\infty$).

As mentioned previously, for large number of data the updated PDF $p(\mathbf{a}|\mathcal{D},\boldsymbol{\delta},\mathcal{M})$ can be approximated by a Gaussian distribution with mean equal to the most probable value $\hat{\mathbf{a}}(\boldsymbol{\delta},\mathcal{D})$ and covariance matrix $\hat{\mathbf{Q}}^{-1}(\boldsymbol{\delta},\hat{\mathbf{a}},\mathcal{D})$, Moreover, asymptotically as $M,N\to\infty$ (i.e., for large number of data) the estimate $\mathbf{S}^M_{y,N}(\omega_k)$ in (9) can be replaced, using the law of large numbers, by its expected value $E[\mathbf{S}_{y,N}(\omega_k)|\mathbf{a}]$ given in (13). Substituting this asymptotic value of the spectral estimate in (10), (16), and (17), the resulting Hessian matrix $\hat{\mathbf{Q}}(\boldsymbol{\delta},\hat{\mathbf{a}},\mathcal{D})\to\mathbf{Q}(\boldsymbol{\delta},\hat{\mathbf{a}})$, with the (j,l) element of the matrix $\mathbf{Q}(\boldsymbol{\delta},\hat{\mathbf{a}})$ given by:

$$Q^{(j,l)}(\boldsymbol{\delta},\hat{\mathbf{a}})=M\sum_{k=k_1}^{k_2}\left[\frac{\partial^2}{\partial a_j\partial a_l}\left\{\mathrm{tr}[\boldsymbol{\lambda}_k(\mathbf{a})\mathbf{S}^M_{y,N}(\omega_k)]+\ln\mu_k(\mathbf{a})\right\}\right]_{\mathbf{a}=\hat{\mathbf{a}}} \tag{19}$$

where $N\to\infty$. It is worth noting that the resulting Hessian matrix $\mathbf{Q}(\boldsymbol{\delta},\hat{\mathbf{a}})$ and the posterior PDF of the parameters a do no longer explicitly depend on the data. The only dependence of $\mathbf{Q}(\boldsymbol{\delta},\hat{\mathbf{a}})$ on the data comes implicitly through $\hat{\mathbf{a}}=\hat{\mathbf{a}}(\boldsymbol{\delta},\mathcal{D})$. Consequently, the information entropy for a given set of data is completely defined by the optimal value $\hat{\mathbf{a}}(\boldsymbol{\delta},\mathcal{D})$ of the model parameters computed for the given data while the spectral density details of the measured data do not enter explicitly in the estimation.

However, since the data are not available, an estimate of the optimal model $\hat{\mathbf{a}}$ cannot be obtained from analysis. Thus, in order to proceed with the design of the optimal sensor configuration, this estimate has to be assumed. In practice, useful designs can be obtained by taking the optimal model $\hat{\mathbf{a}}$ to be a nominal model $\mathbf{a}_0$ chosen by the designer to be representative of the system. In this case, the entropy measure in (18) takes the form (for large N),

$$H_{\mathbf{a}|\mathbf{a}_0}(\boldsymbol{\delta})=\frac{1}{2}N_a[\ln(2\pi)+1]-\frac{1}{2}\ln\det\mathbf{Q}(\boldsymbol{\delta},\mathbf{a}_0) \tag{20}$$

which depends on the sensor configuration vector $\boldsymbol{\delta}$ and the chosen parameters $\mathbf{a}_0$ of the nominal model. The optimal sensor configuration given the nominal model $\mathbf{a}_0$ is chosen as the one that minimizes this information entropy measure over all possible configurations. Genetic algorithms [15] can be used to solve the resulting discrete optimization problem.

The optimal sensor configuration estimates obtained by minimizing (20) depend on the designer's choice of the best model $\mathbf{a}_0$. One way to quantify and account for the uncertainty in the nominal model $\mathbf{a}_0$ is to use a prescribed PDF $p(\mathbf{a}_0)$ of $\mathbf{a}_0$. In this case, the problem of optimal sensor configuration becomes the one of minimizing the information entropy $H_{\mathbf{a},\mathbf{a}_0}(\boldsymbol{\delta})=E_{\mathbf{a},\mathbf{a}_0}[-\ln p(\mathbf{a},\mathbf{a}_0|\boldsymbol{\delta},\mathcal{M})]$ which is a measure of the overall uncertainty in both $\mathbf{a}$ and $\mathbf{a}_0$. Using the fact that $p(\mathbf{a},\mathbf{a}_0|\boldsymbol{\delta},\mathcal{M})=p(\mathbf{a}|\mathbf{a}_0,\boldsymbol{\delta},\mathcal{M})p(\mathbf{a}_0)$, it can be readily shown that this problem is equivalent to minimizing the quantity

$$h(\boldsymbol{\delta})=\frac{1}{2}N_a[\ln(2\pi)+1]-\frac{1}{2}\int\ln\det\mathbf{Q}(\boldsymbol{\delta},\mathbf{a}_0')p(\mathbf{a}_0')d\mathbf{a}_0' \tag{21}$$

with respect to $\boldsymbol{\delta}=[\delta_1,\ldots,\delta_{N_d}]^T$. Note that the information entropy $H_{\mathbf{a}|\mathbf{a}_0}(\boldsymbol{\delta})$ given by (20) is a special case of $h(\boldsymbol{\delta})$ in (21) corresponding to the choice $p(\mathbf{a}_0')=\delta(\mathbf{a}_0'-\mathbf{a}_0)$, where $\delta(\mathbf{a})$ denotes the delta function. The multi-dimensional integration over $\mathbf{a}_0'$ involved in computing (21) can be carried out approximately but efficiently using an asymptotic expansion developed to treat these types of integrals [16].

The present formulation of the optimal sensor location problem in terms of the information entropy provides a rational procedure for comparing the uncertainty of the estimates of the parameter values for different sensor configurations. Specifically, a direct measure of the uncertainty reduction is provided by the change $h(\boldsymbol{\delta})-h_0(\boldsymbol{\delta}_0)$ of the information entropy, where $h(\boldsymbol{\delta})$ and $h_0(\boldsymbol{\delta}_0)$ represent respectively the information entropy for a sensor configuration $\boldsymbol{\delta}$ and a reference sensor configuration δ_0. It should be noted that the reference sensor configuration $\boldsymbol{\delta}_0$ may correspond to different number of sensors than those in the configuration vector $\boldsymbol{\delta}$. Equivalently, the reduction in uncertainty can also be quantified by the parameter-uncertainty ratio defined by [17]

$$\frac{s}{s_0}=\exp\left[\frac{h(\boldsymbol{\delta})-h_0(\boldsymbol{\delta}_0)}{N_a}\right] \tag{22}$$

where s and s_0 represent a measure of the spread of the PDF of $\mathbf{a}$ about its most probable value for the sensor configuration cases $\boldsymbol{\delta}$ and $\boldsymbol{\delta}_0$, respectively. The smaller the value of the parameter uncertainty ratio, the smaller the uncertainty in the parameter estimates.

4 Application

4.1 Example 1: 8 DOFs Chain-Like System. The methodology is applied to a structure represented by an 8-DOF chain mass-spring model, shown in Fig. 1, with one end of the chain fixed at the base and the other end left free. The spring stiffness to mass ratio for the nominal structure is chosen to be $k_0/m_0=1160\ \mathrm{s}^{-2}$ for each of the mass-spring link so that the fundamental modal frequency of the structure is 1.00 Hz. Classical normal modes are assumed with the modal damping fixed at 5% for all modes.

The objective is to design an optimal sensor configuration for the purpose of updating the model of the structure as well as monitoring the condition (health) of the structure using measured response data only. The measured response time histories are accelerations recorded at one to eight DOFs. The unmeasured excitation is considered to be a base excitation. This base excitation case is useful for the design of sensor configuration for the purpose of model updating and health monitoring of shear models of building structures subjected to uncertain earthquake excitations. The spring stiffnesses and masses shown in Fig. 1 represent the interstory stiffnesses and floor masses of the building. It is worth noting that the base excitation case is equivalent to the case of fully-correlated forces applied at all eight DOFs of a fixed-base structure. Thus, the results reported in the numerical study that follows will also be useful for the design of sensor configuration for the purpose of model updating and health monitoring of chain-like structures (such as shear models of buildings) subjected to unmeasured wind loads.

Emphasizing earthquake applications, it is assumed that the uncertain base excitation will have a spectral density which is represented by the well-known Clough-Penzien spectrum:

$$S_g(\omega)=\frac{S_0\left[1+4\zeta_g^2\left(\frac{\omega}{\omega_g}\right)^2\right]\left(\frac{\omega}{\omega_f}\right)^4}{\left[\left(1-\left(\frac{\omega}{\omega_g}\right)^2\right)^2+4\zeta_g^2\left(\frac{\omega}{\omega_g}\right)^2\right]\left[\left(1-\left(\frac{\omega}{\omega_f}\right)^2\right)^2+4\zeta_f^2\left(\frac{\omega}{\omega_f}\right)^2\right]} \tag{23}$$

where the parameters have fixed values given by $S_0=0.03512m^2\ \mathrm{s}^{-3}$, $\omega_f=0.5\pi$, $\omega_g=5\pi$ and $\zeta_f=\zeta_g=0.6$. The measured quantities are digitized absolute accelerations recorded over a time interval $T_0=10$ s with sampling interval $\Delta t=0.01$ s.

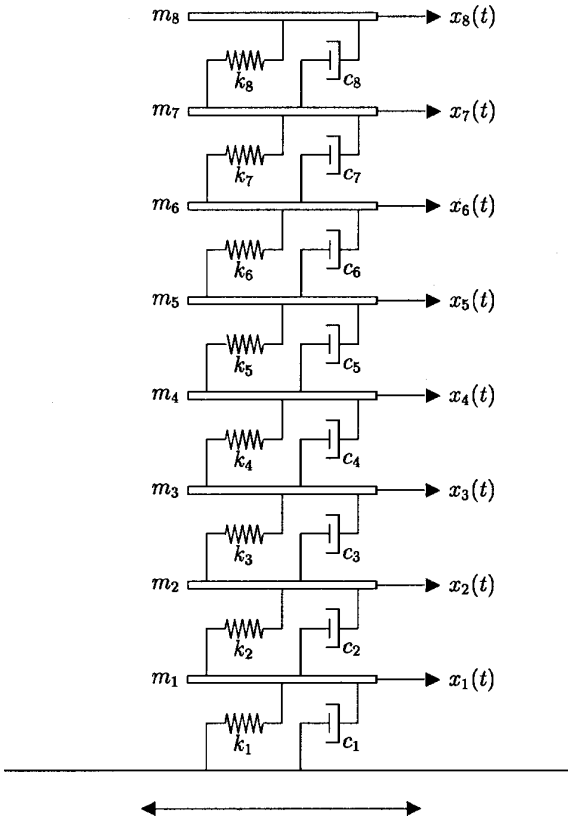

Fig. 1 8-DOF chain spring-mass structure

4.1.1 Overall Results. In order to investigate the effects of structural parameterization on the optimal sensor location, results are presented for the following three cases, designated by Cases A, B, and C. In Case A, two model parameters $\boldsymbol{\theta}=(\theta_1,\theta_2)$ are considered by dividing the structure into two substructures with spring stiffnesses $k_1=k_2=k_3=k_4=\theta_1 k_0$ and $k_5=k_6=k_7=k_8=\theta_2 k_0$. That is, the uncertainty in the stiffness is assumed to be fully correlated for the first four stories and the last four stories. In Case B, only four uncertain parameters $\boldsymbol{\theta}=(\theta_1,\theta_2,\theta_3,\theta_4)$ are considered by dividing the structure into four substructures with spring stiffnesses $k_1=k_2=\theta_1 k_0$, $k_3=k_4=\theta_2 k_0$, $k_5=k_6=\theta_3 k_0$ and $k_7=k_8=\theta_4 k_0$. In Case C, eight uncertain parameters $\boldsymbol{\theta}=(\theta_1,\ldots,\theta_8)$ are considered, one for each spring stiffness, so that $k_i=\theta_j k_0$, $j=1,\ldots,8$.

As a first case, the effects of different levels of measurement noise and modeling error have been considered by taking the rms of the prediction error at each measured DOF to be equal to 10% and 20% of the rms of the response at the corresponding DOF. It was found that the optimal sensor locations are insensitive to the two values of the noise level assumed [17]. Therefore, results are next presented only for the case of prediction error fixed at 10%.

Figures 2, 3, and 4 show the variation of the uncertainty in the estimate of the parameter set $\boldsymbol{\theta}$ as a function of the number of observed modes and number of sensors placed at the optimal locations for Cases A, B, and C, respectively. The ratio s/s_0, defined in (22), is used to measure this uncertainty, where the reference sensor configuration $\boldsymbol{\delta}_0$ is chosen to correspond to the optimal sensor configuration case for which all eight DOFs of the structure are instrumented with sensors and all eight modes of the structure are observable. Results of the ratio s/s_0 are also presented in Figs. 2, 3, and 4 for the worst possible sensor locations. The results for the ratio s/s_0 are presented for increasing numbers of observable modes.

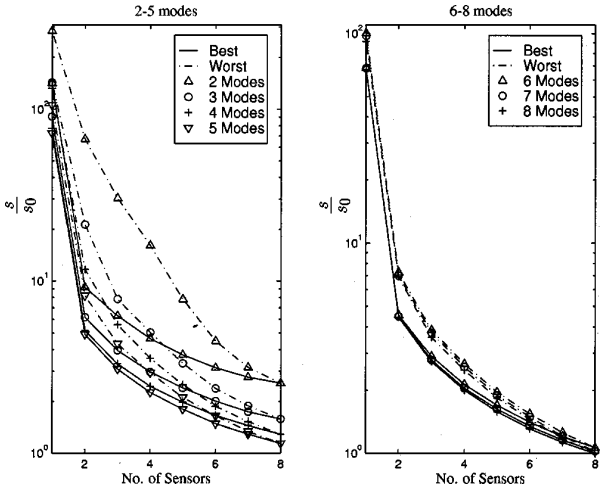

Fig. 2 Values of s/s_0 for different number of modes (Case A)

It is observed that for any given number of modes, the value of s/s_0, and thus the uncertainty in the prediction of the value of $\boldsymbol{\theta}$, is reduced as additional sensors are placed in the structure. Similarly, for any given number of sensors, the uncertainty in the value of the model parameters is reduced as additional modes are observable in the response. The observed variation of s/s_0 with the number of sensors or the number of observable modes is expected since increasing the number of sensors and/or the number of modes has an effect of extracting more information from the data which corresponds to lower values of s/s_0. When too few sensors are used and/or too few modes are observed, the model parameters are essentially unidentifiable or almost unidentifiable [12,18] which is reflected in the very large values of s/s_0.

It should be noted that the difference $(s_{\text{opt}}-s_{\text{worst}})/s_0$ between the values of s/s_0 computed at the optimal and worst sensor locations is a direct measure of the maximum improvement that can be achieved by optimally placing the sensors in a structure. This difference can be seen in Figs. 2, 3, and 4 to decrease monotonically with increasing number of sensors and becomes relatively small as the number of sensors approaches the number of DOFs. It is also observed from these figures that the difference decreases as the number of observable modes increases. These results clearly

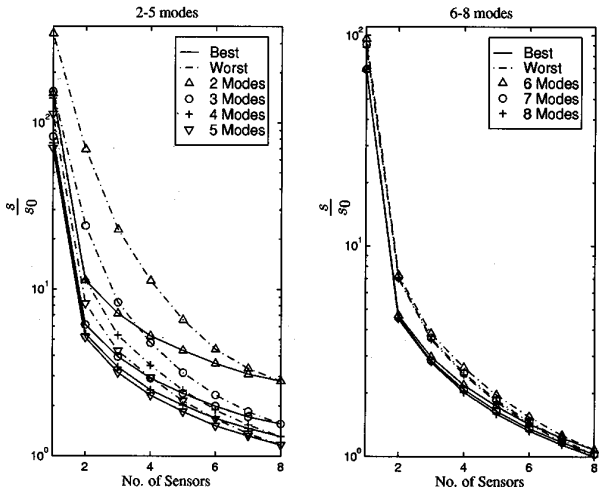

Fig. 3 Values of s/s_0 for different number of modes (Case B)

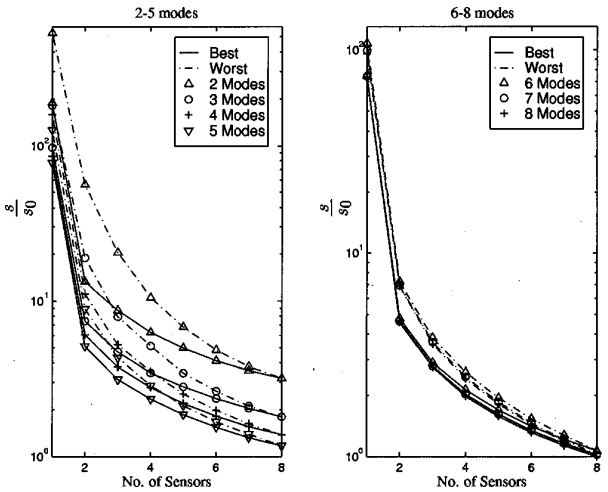

Fig. 4 Values of s/s_0 for different number of modes (Case C)

indicate that optimizing the location of the sensors in the structure is of particular importance, especially for a relatively small number of sensors and/or small number of observable modes as compared to the number of DOFs.

It is clear from Figs. 2, 3, and 4 that a given number of sensors placed at their optimal configuration may yield estimates of the model parameters which are much better than the ones obtained by a larger number of sensors arbitrarily placed in the structure. For example, for Cases A, B, and C and for up to 3 observable modes, two sensors placed at their optimal location will provide a better estimate than three sensors placed at the worst location. Thus, optimizing the sensor location in a structure is equivalent to optimizing the cost of instrumentation.

In experimental design, the proposed methodology could be used as a rational procedure for evaluating and weighing the benefits of adding more sensors in the structure against the benefits of exciting and measuring more modes using the existing number of sensors. For example, consider Case C for which there are 3 sensors placed in the structure and 2 observable modes. The value of the parameter-uncertainty ratio s/s_0, given in Fig. 4, for this case is 8.7. Exciting and observing one more mode (third mode) results in an improved quality of the parameter estimation corresponding to a lower ratio value of 4.7. To achieve approximately the same quality in the estimates of the model parameters using additional sensors with the original two modes, one needs to add at least 4 more sensors in the structure to get a reduction of the information entropy to the ratio level of 3.6. Given now that a third mode is excited and observed with three sensors, the quality in the prediction can be improved further by adding a fourth sensor than exciting and observing one additional mode.

Thus, the proposed method can guide the design of the experiment with respect to which direction to proceed in improving the quality of the estimates. The final decision on whether to use more sensors or excite and observe more modes will depend on the number of sensors available and their cost, as well as the feasibility and cost of exciting and measuring more modes.

The optimal sensor locations for Cases A, B, and C are given in Tables 1, 2, and 3, respectively. Comparing the optimal sensor location results for Cases A, B, and C it is concluded that the optimal location of the sensors depends on the number of sensors placed on the structure, number of modes observed, and the structural parameterization scheme employed. As an illustrative example, consider finding the optimal locations of four sensors for Case B. The results for Case B shown in Table 2 indicate that two sensors should always be placed at the second and fourth floor, while the exact locations of the other two sensors depend on the number of observable modes contributing significantly to the response. It is worth mentioning that for the case of three observable modes the optimal sensor configuration (2, 4, 5, 8) corresponds to a value of the uncertainty ratio s/s_0 which is almost the same as the value for the suboptimal sensor configuration (2, 4, 6, 8). Noting that the sensor configuration (2, 4, 6, 8) is optimal for the case of two, four, five and six observable modes, it can be argued that the preferable location for the third sensor is the 6th floor, independent of the number of observable modes. The preferred location for the fourth sensor is the 8th floor for the case where up to six modes are observable and the 3rd floor for the case where the 7th and/or the 8th modes are observable. Similar arguments can be stated for the other cases presented in these tables.

Comparing Case B and Case C, it can be seen that the optimal sensor locations for Case C are at the lower floors of the building than it is for Case B. Note also that the optimal locations for (N_0+1) sensors does not always contain the optimal locations for N_0 sensors as a subset.

Table 1 Optimal sensor configuration (Case A)

	No. of Sensors						
No. of modes	1	2	3	4	5	6	7
2	3	4 8	4 5 8	3 4 7 8	3 4 6 7 8	1 2 3 4 5 6	2 3 4 5 6 7 8
3	8	4 8	3 5 8	2 4 5 8	2 4 5 6 8	2 3 4 5 6 8	2 3 4 5 6 7 8
4	6	3 6	2 4 6	2 4 6 8	2 4 5 6 8	2 3 4 5 6 8	2 3 4 5 6 7 8
5	8	2 4	4 6 8	3 5 6 8	2 4 5 6 8	2 3 4 5 6 8	1 2 3 4 5 6 8
6	4	2 4	4 6 8	3 4 6 8	3 4 5 6 8	2 3 4 5 6 8	2 3 4 5 6 7 8
7	4	2 4	3 5 7	3 4 6 8	3 4 5 6 8	2 3 4 5 6 8	2 3 4 5 6 7 8
8	4	2 4	3 5 7	2 3 4 6	2 3 4 5 6	2 3 4 5 6 7	2 3 4 5 6 7 8

Table 2 Optimal sensor configuration (Case B)

	No. of Sensors						
No. of modes	1	2	3	4	5	6	7
2	2	2 6	2 5 8	2 4 6 8	2 4 5 6 8	2 3 4 6 7 8	2 3 4 5 6 7 8
3	8	4 8	3 5 8	2 4 5 8	2 4 5 6 8	2 3 4 5 6 8	2 3 4 5 6 7 8
4	8	3 6	2 4 8	2 4 6 8	2 4 5 6 8	2 3 4 5 6 8	2 3 4 5 6 7 8
5	8	2 4	2 4 8	2 4 6 8	2 4 5 6 8	2 3 4 5 6 8	1 2 3 4 5 6 8
6	8	2 4	2 4 8	2 4 6 8	2 3 4 6 8	2 3 4 5 6 8	2 3 4 5 6 7 8
7	8	2 4	2 4 6	2 3 4 6	2 3 4 6 8	2 3 4 5 6 8	1 2 3 4 5 6 8
8	8	2 4	2 4 6	2 3 4 6	2 3 4 5 6	2 3 4 5 6 8	1 2 3 4 5 6 8

4.1.2 Sensitivity to Uncertainty in the Nominal Model. Next, the effect of nominal model uncertainties on the optimal sensor locations is investigated for Case A of two parameters. Only one uncertain parameter θ_1 is assumed while the nominal value of the other parameter θ_2 is taken to be fixed at $\theta_2=1$. Specifically, the uncertainty in the parameter θ_1 is quantified by a uniform PDF. Different levels of uncertainties are simulated by varying the coefficient of variation (COV) from 0.0, corresponding to no uncertainty in the nominal model, to 0.5, corresponding to relatively large levels of uncertainties. Optimal sensor configuration design corresponding to large uncertainties is applicable to the case encountered in structural health monitoring applications since in the design one should account for an unknown, often large, level of structural damage. Optimal sensor design for relatively small levels of uncertainties is applicable to the case encountered in model updating applications since a pretest finite-element model is usually available and thus one should take into account a relatively small level of uncertainty in the pre-test (nominal) model.

Tables 4 and 5 show, respectively, the optimal and worst sensor locations for up to 5 sensors and for up to 2, 4, and 8 observable modes, respectively, as a function of the COV of the uncertain parameter θ_1. Figures 5, 6, and 7 show the corresponding optimal and worst values of s/s_0 as a function of the number of sensors for 2, 4, and 8 observable modes, respectively. The results have been obtained using (21) and (22) with h_0 chosen for all cases to correspond to the value computed for COV=0.0, 8 modes, and 5 sensors placed at the optimal configuration. The difference $(s_{\text{opt}}-s_{\text{worst}})/s_0$ in Figs. 5, 6, and 7 is a direct measure of the maximum improvement that can be achieved by optimizing the sensor configuration in a structure. For a given number of sensors and/or given number of modes, the reduction in s/s_0 as a function of COV of θ_1 is small as compared to the difference $(s_{\text{opt}}-s_{\text{worst}})/s_0$ which clearly indicates that the values of s/s_0 are insensitive to the level of uncertainty in θ_1.

The results in Table 4 clearly show that the optimal configuration is relatively insensitive to the level of uncertainty. Some sensitivity is observed for relatively high (COV=0.5) levels of uncertainties. However, this sensitivity to the value of COV is not important since the corresponding values of s/s_0 for different COV are found to be very close which means that both instrumentation strategies are almost equally optimal. As a result, the instru-

Table 3 Optimal sensor configuration (Case C)

	No. of Sensors						
No. of modes	1	2	3	4	5	6	7
2	2	3 7	2 4 7	2 3 6 7	2 3 5 7 8	2 3 4 6 7 8	2 3 4 5 6 7 8
3	8	4 8	2 5 8	2 4 5 8	2 3 4 5 8	2 3 4 5 6 8	1 2 3 4 5 6 8
4	8	3 6	1 3 6	1 3 5 8	1 2 4 5 8	1 2 3 4 5 8	1 2 3 4 5 6 8
5	8	1 3	1 3 6	1 3 5 6	1 2 3 4 6	1 2 3 4 5 8	1 2 3 4 5 6 8
6	4	2 4	1 3 5	1 2 3 5	1 2 3 4 5	1 2 3 4 5 7	1 2 3 4 5 6 8
7	4	2 4	1 3 5	1 2 3 5	1 2 3 4 5	1 2 3 4 5 6	1 2 3 4 5 6 7
8	4	2 4	1 3 5	1 2 3 5	1 2 3 4 5	1 2 3 4 5 6	1 2 3 4 5 6 7

Table 4 Optimal sensor configuration (large uncertainty)

		No. of Sensors				
No. of modes	COV	1	2	3	4	5
2	0.0	3	4 8	4 5 8	3 4 7 8	3 4 6 7 8
	0.1	3	4 8	4 5 8	3 4 7 8	3 4 6 7 8
	0.3	3	4 8	3 5 8	3 4 7 8	3 4 6 7 8
	0.5	3	4 7	3 5 8	3 5 7 8	3 4 5 7 8
4	0.0	6	3 6	2 4 6	2 4 6 8	2 4 5 6 8
	0.1	6	3 6	2 4 6	2 4 6 8	2 4 5 6 8
	0.3	8	2 4	2 4 6	2 4 5 8	2 4 5 6 8
	0.5	8	2 5	2 4 5	2 4 5 8	2 4 5 6 8
8	0.0	4	2 4	3 5 7	2 3 4 6	2 3 4 5 6
	0.1	4	2 4	3 4 6	2 3 4 6	2 3 4 5 6
	0.3	4	2 4	3 4 6	2 3 4 6	2 3 4 5 6
	0.5	3	3 5	3 4 6	2 3 4 5	2 3 4 5 6

Table 5 Worst sensor configuration (large uncertainty)

		No. of Sensors				
No. of modes	COV	1	2	3	4	5
2	0.0	6	1 2	1 2 3	1 2 3 4	1 2 3 4 5
	0.1	6	1 2	1 2 3	1 2 3 4	1 2 3 4 5
	0.3	6	1 2	1 2 3	1 2 3 4	1 2 3 4 5
	0.5	6	1 2	1 2 3	1 2 3 4	1 2 3 4 5
4	0.0	7	1 2	1 2 7	1 2 7 8	1 2 3 7 8
	0.1	7	1 2	1 2 7	1 2 7 8	1 2 3 7 8
	0.3	3	1 2	1 2 7	1 2 7 8	1 2 3 7 8
	0.5	3	1 2	1 2 3	1 2 7 8	1 2 6 7 8
8	0.0	2	1 8	1 2 8	1 2 7 8	1 2 6 7 8
	0.1	2	1 8	1 7 8	1 2 7 8	1 2 6 7 8
	0.3	2	1 8	1 7 8	1 6 7 8	1 2 6 7 8
	0.5	7	6 7	6 7 8	5 6 7 8	1 2 6 7 8

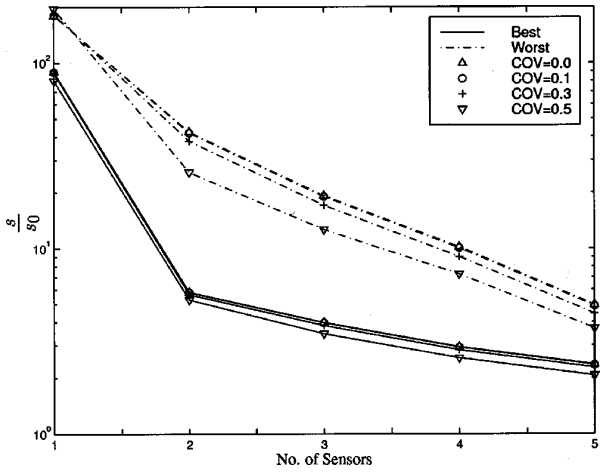

Fig. 5 Values of s/s_0 for different values of COV (2 modes)

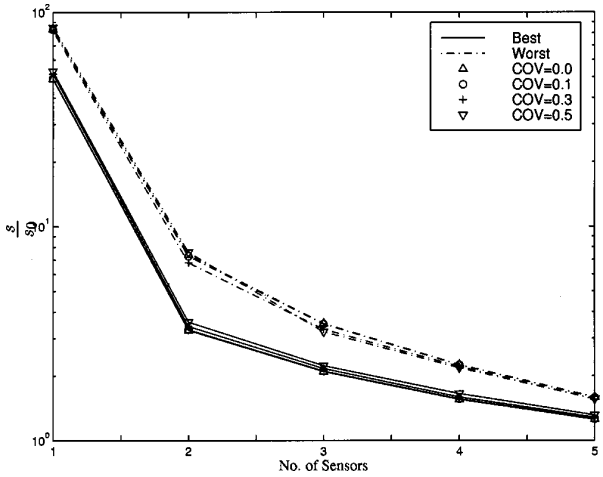

Fig. 6 Values of s/s_0 for different values of COV (4 modes)

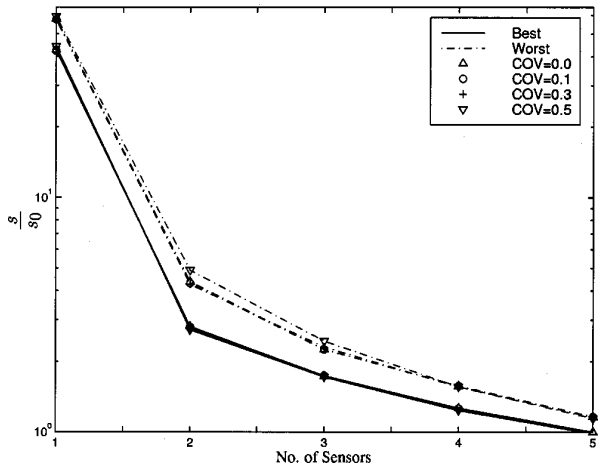

Fig. 7 Values of s/s_0 for different values of COV (8 modes)

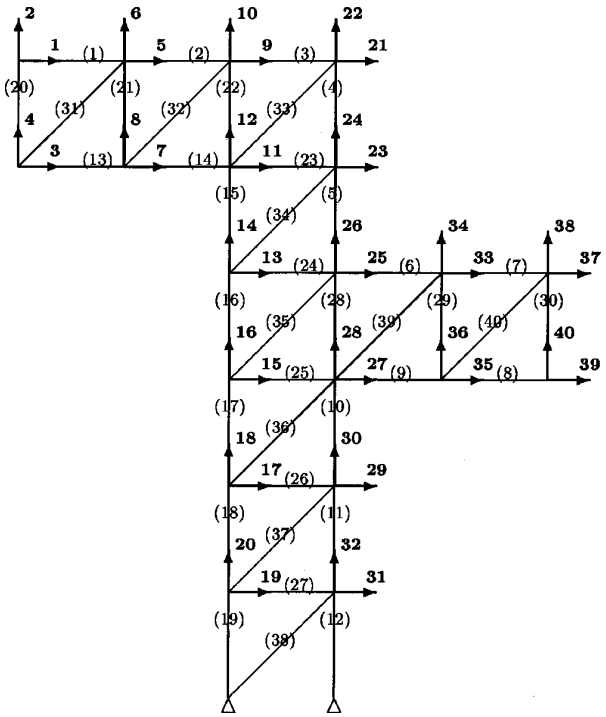

Fig. 8 40-DOF Truss model

mentation designed to be optimal for the case of COV=0 is also almost optimal for the case of COV≠0. This result is also true in the case for which the uncertain parameter is taken to be θ_2.

4.2 Example 2: 40-DOF Truss Model. The second example refers to the truss model shown in Fig. 8 where it is assumed that accelerations can be measured. The length of all the horizontal and vertical members is equal to 3.0 m. All members have the same cross sectional area $A=0.01\ \text{m}^2$. The mass density is $\rho=7860\ \text{kg/m}^3$ and the nominal stiffness is $k_0=EA/L=125.6\ \text{MN/m}$. The first ten nominal natural frequencies are 2.00 Hz, 6.51 Hz, 9.36 Hz, 14.88 Hz, 18.18 Hz, 28.84 Hz, 36.25 Hz, 42.57 Hz, 47.06 Hz, and 51.01 Hz, respectively. Rayleigh damping is assumed, that is, $\mathbf{C}=\alpha\mathbf{M}+\beta\mathbf{K}$, where the nominal value for α and β are $0.192\ \text{s}^{-1}$ and 3.73×10^{-4} s, respectively. As a result, the damping ratios are 1% for the first two modes. The total measured time is 60.0 s with $\Delta t=0.002$ s. The stiffness parameters are separated into four groups as follows: $k_j=\theta_1 k_0$, $j=1,2,\ldots,12$, $k_j=\theta_2 k_0$, $j=13,14,\ldots,19$, $k_j=\theta_3 k_0$, $j=20,21,\ldots,30$ and $k_j=\theta_4 k_0/\sqrt{2}$, $j=31,32,\ldots,40$. The first two groups consist of the outer elements, which contribute mainly to bending. The third group consists of all the inner vertical and horizontal elements and the fourth group consists of all the diagonal elements, which contribute mainly to the shear. In this example, seven uncertain parameters are considered: the four stiffness parameters θ_j, $j=1,2,3,4$, the spectral intensity of the excitation and the damping coefficients α and β.

Two cases are investigated corresponding to different excitation patterns:

(a) an independent band-limited Gaussian white noise excitation at all DOFs, which simulates wind excitation.
(b) a horizontal band-limited Gaussian white noise excitation at the base, which simulates earthquake ground shaking.

It is found that one sensor only gives an unidentifiable case independently of the location of the sensor. This means that only one sensor is not enough for the estimation of all seven structural

Table 6 Optimal sensor configurations and their associated entropy values

Case	No. of Sensors	$\boldsymbol{\delta}_1$	H_1	$\boldsymbol{\delta}_2$	H_2	$\boldsymbol{\delta}_3$	H_3
A	2	5 11	−50.5935	9 11	−50.4130	11 33	−49.2953
	3	5 7 23	−51.7564	3 9 11	−51.6345	5 11 25	−51.4070
	4	5 7 21 23	−52.6697	5 7 23 25	−52.4158	5 7 21 25	−52.3680
	5	5 7 21 23 25	−53.1784	5 7 21 23 27	−53.0620	5 7 21 23 33	−53.0043
B	2	5 11	−67.0392	9 11	−66.9114	11 33	−65.7316
	3	5 7 23	−68.1850	3 9 11	−68.0830	5 11 25	−67.8465
	4	5 7 21 23	−69.0769	5 7 23 25	−68.7910	5 7 21 25	−68.7572
	5	5 7 21 23 25	−69.5623	5 7 21 23 27	−69.4157	5 7 21 23 33	−69.3964

and excitation parameters. Also, it was found that for the configuration cases corresponding to five sensors, there exist many sensor configurations which correspond to an unidentifiable case. Therefore, the optimal placement of sensors is essential because an arbitrary placement of sensors might lead to an unidentifiable case, in which some parameters cannot be identified.

Table 6 shows the best (optimal), the second best and the third best sensor configurations and the associated entropy values for two to five sensors assuming that 10 modes are excited and observed. It is worth noting that the optimal sensor configurations are identical using two to five sensors for both Cases A and B, implying that the optimal sensor locations are robust to the selected excitation patterns. Furthermore, for the same sensor configuration, Case B gives smaller entropy (better parameter estimates) than Case A. This seems somewhat surprising at first since one might expect that the excitation pattern of Case A can excite more higher modes than that of Case B. However, these higher modes are mainly very local modes and are not included in the ten modes considered. Furthermore, the excitations in Case A counteracts one another for the very low modes. On the other hand, the excitation pattern in Case B produces a very strong input for the very low modes. Therefore, Case B provides much better parameter estimations than Case A. In addition, one can observe that all the optimal sensor locations are at the horizontal DOFs because the very low modes are primarily in a horizontally swaying type of motion.

It is also worth noting that although the location "11" is included in the best three sensor configurations when using two sensors, it is not included in the optimal sensor locations when using three sensors. In general, it has been observed that the optimal sensor locations corresponding to N_0 sensors do not necessary include all the locations in the optimal sensor configurations corresponding to N_0-1 sensors. In fact, the different channels of the measurements at the optimal sensor configuration contain information that is complementary to one another.

The computational cost required for computing optimal sensor configuration corresponding to more than a few sensors become excessive for large structures in the sense that the number of possible sensor configurations to be searched for optimality is extremely large. Genetic algorithms [15] are the most-suited computational tools for solving the discrete optimization problem of finding the optimal sensor positions. In particular, genetic algorithms explore a fraction of all possible sensor configurations and provide an almost optimal sensor configuration with computational cost several orders of magnitude less than the cost required to examine all possible sensor configurations.

5 Conclusions

The methodology proposed in this study is useful for designing cost-effective optimal sensor configurations such that the corresponding measured data are most informative about the condition of the structure. The methodology was developed for the case where the excitation is not measured, a case often encountered in model updating and health monitoring applications from ambient vibration data. It is demonstrated that optimizing the sensor configuration is important and useful for the case of a relatively small number of sensors and small number of observable modes as compared to the number of the model DOFs.

The methodology has been extended to treat the case for which the nominal model, on which the optimal sensor configuration estimate was based, is uncertain. The optimal sensor configuration is found to be insensitive to relatively large uncertainties in the nominal model. This result is extremely useful in health monitoring applications since the optimal sensor configuration obtained in the design stage using a nominal model representative of the undamaged structure, remains almost optimal even when the structure has been changed considerably due to significant and uncertain damage. It is equally useful in model updating applications in which the updated model may not be close to the nominal model, usually finite-element model, used for the design of the sensor configuration.

The technique can be extended to design and optimize a sensor configuration that takes into account robustness issues related to sensor failure due to miss-calibration, de-bounding and bad readings commonly encountered when large structures are instrumented. Also, it can be used to upgrade an existing array of sensors by finding the optimal location of an additional array of sensors given the existing configuration.

Acknowledgments

This research was funded by the Greek General Secretariat of Research and Technology and the European Community Fund within the PENED 99 program framework under grant 99ED580, and the Hong Kong Research Grant Council under grant HKUST 6253/ooE. This support is gratefully acknowledged.

References

[1] Cobb, R. G., and Liebst, B. S., 1996, "Sensor location prioritization and structural damage localization using minimal sensor information," AIAA J., **35**, No. 2, pp. 369–374.
[2] Hemez, F. M., and Farhat, C., 1994, "An energy based optimum sensor placement criterion and its application to structural damage detection," *Proc. 12th IMAC, Society of Experimental Mechanics, Honolulu*, pp. 1568–1575.
[3] Heredia-Zavoni, E., Montes-Iturrizaga, R., and Esteva, L., 1999, "Optimal instrumentation of structures on flexible base for system identification," Earthquake Eng. Struct. Dyn., **28**, No. 12, pp. 1471–1482.
[4] Shi, Z. Y., Law, S. S., and Zhang, L. M., 2000, "Optimum sensor placement for structural damage detection," J. Eng. Mech., **126**, No. 11, pp. 1173–1179.
[5] Udwadia, F. E., 1994, "Methodology for optimal sensor locations for parameters identification in dynamic systems," J. Eng. Mech., **120**, No. 2, pp. 368–390.
[6] Heredia-Zavoni, E., and Esteva, L., 1998, "Optimal instrumentation of uncertain structural systems subject to earthquake motions," Earthquake Eng. Struct. Dyn., **27**, pp. 343–362.
[7] Papadimitriou, C., Beck, J. L., and Au, S. K., 2000, "Entropy-based optimal sensor location for structural model updating," J. Vib. Control, **6**, No. 5, pp. 781–800.
[8] Jaynes, E. T., 1978, *Where do we stand on maximum entropy?* MIT Press, Cambridge.
[9] Conte, J. P., and Krishnan, S., 1995, "Modal identification method for structures subjected to unmeasured random excitations," *Proceedings of the 10th ASCE Engineering Mechanics Specialty Conference*, pp. 1296–1299, University of Colorado at Boulder, Boulder, Colorado, May.
[10] Yuen, K.-V., and Katafygiotis, L. S., 2001, "Bayesian time-domain approach for modal updating using ambient data," Probab. Eng. Mech., **16**, No. 3, pp. 219–231.

[11] Katafygiotis, L. S., and Yuen, K.-V., 2001, "Bayesian spectral density approach for modal updating using ambient data," Earthquake Eng. Struct. Dyn., **30**, No. 8, pp. 1103–1123.
[12] Beck, J. L., and Katafygiotis, L. S., 1998, "Updating models and their uncertainties. I: Bayesian statistical framework," J. Eng. Mech., **124**, No. 4, pp. 455–461.
[13] Yuen, K.-V., 1999, "Structural modal identification using ambient dynamic data," MPhil thesis, Technical report, Hong Kong University of Science and Technology, Hong Kong.
[14] Krishnaiah, P. R., 1976, "Some recent developments on complex multivariate distributions," J. Multivariate Anal., **6**, pp. 1–30.
[15] Goldberg, D. E., 1989, *Genetic Algorithms in Search, Optimization and Machine Learning*. Allison Wesley.
[16] Papadimitriou, C., Beck, J. L., and Katafygiotis, L. S., 1997, "Asymptotic expansions for reliability and moments of uncertain systems," J. Eng. Mech., **123**, No. 12, pp. 1219–1229.
[17] Katafygiotis, L. S., Papadimitriou, C., and Yuen, K.-V., 1999, "An optimal sensor location methodology for designing cost-effective modal experiments," *EURODYN' 99*, pp. 617–622, Prague, Czech Republic.
[18] Katafygiotis, L. S., Lam, H. F., and Papadimitriou, C., 2000, "Treatment of unidentifiability in structural model updating," Adv. Struct. Eng., **3**, No. 1, pp. 19–39.